

# Regrasping on Printed Circuit Boards with the Smart Suction Cup

Jungpyo Lee<sup>1</sup>, Zheng Sun<sup>2</sup>, Zhipeng Dong<sup>2</sup>, Fei Chen<sup>2</sup>, Hannah S. Stuart<sup>1</sup>

**Abstract**—The disposal of waste electrical and electronic equipment (WEEE) presents a sustainability challenge, particularly for waste printed circuit boards (PCBs). PCBs are challenging to sort out from other waste materials in part because traditional industrial end-effectors struggle to reliably grip these irregularly shaped objects with unmodeled surface-mounted components. Vision-based separators, while effective for object categorization, face challenges with identifying precise grasp points on PCB surfaces. This paper studies regrasping control to enhance suction cup grasping performance on PCBs, addressing issues arising from uneven surfaces and intricate features that interfere with suction sealing. We categorize PCBs into two recycling levels – with large surface features intact or removed – and conduct experiments on both stationary and conveyor belt setups with realistic vision-based grasp planners. Results show that jumping regrasping improves pick-and-place success rate. Haptically driven jumping – using the Smart Suction Cup – is especially useful for unprocessed waste PCBs with large surface mount parts. The proposed method offers a promising solution to enhance the efficiency and reliability of robotic grasping in recycling applications.

## I. INTRODUCTION

As of now, many waste printed circuit boards (PCBs) are not recycled [1], [2] and the rapid global growth of electronics industries has led to a surge in electronic waste [3], [4]. Resulting pollution harms both local ecosystems and the human populations residing in proximity to primary recycling facilities [5], [6]. PCBs present especially intricate designs with high metal contents and potential toxicity, making automated high-volume PCB recycling both difficult and important. The irregular shapes and sizes of PCBs with unmodeled surface mounted components makes reliable gripping difficult with conventional industrial end-effectors. Thus, sorting PCBs out from other waste materials using a pick-and-place process remains a bottleneck. Modern robotic manipulation technology suitable for PCB handling therefore has the potential to improve waste management practices.

Suction cups, also known as vacuum grippers, play a crucial and versatile role in various industrial robot applications [9] [10]; they are fast, reliable, affordable, and effective on smooth, flat, and/or lightweight objects. Suction cups already enable the pick-and-place of some recyclable items [11], and facilitate the integration of robots into industrial recycling sorting applications [12], [13]. For objects that are too bumpy or difficult for suction cups to grip consistently, opposable

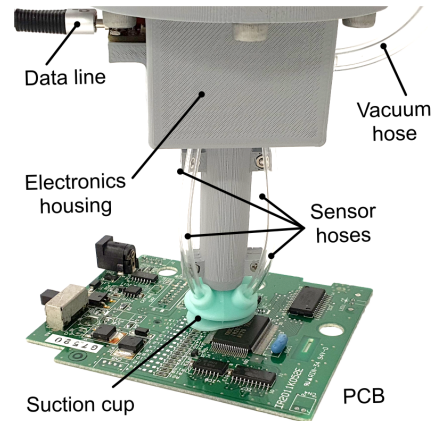


Fig. 1: The multi-chamber Smart Suction Cup – equipped with four internal chambers, each linked to a pressure transducer for monitoring internal flow rate [7], [8] – touches a PCB on the edge of a surface mounted integrated circuit. The gripper can detect minor seal disruptions caused by physical interaction with such surface irregularities.

grippers and multi-fingered hands enable fine adaptation to varied object shapes [14], [15]. However, suction grippers are typically simpler and cheaper in comparison to other articulated end-effectors. Our goal is to expand the capabilities of suction cups to grip irregular surfaces so that more complex end-effector hardware is not required.

Vision-based separator technology enables the identification of different mixed waste for sorting [16]. While vision-based planners have proven effective for object grasping, challenges arise when dealing with uneven surfaces and intricate features on objects [17]. PCBs, in particular, pose difficulties for vision-based systems due to their complex array of small electronic components and vias, rendering suction performance difficult to predict accurately. This is especially true for fast-throughput conveyor systems, where the constantly moving belt may not provide enough time for the vision system to fully capture and process all the intricate features on the PCBs that affect suction cup gripper success. We therefore aim to provide fast, successful suction cup gripping on PCBs without accurate visual predictions or models of surface geometry.

### A. Prior Work

In our previous work, Huh et al. (2021) introduced a custom-molded multi-chamber smart suction cup gripper capable of measuring four distinct pressure values corresponding to the sealing of individual chambers [7]. This cup is depicted in Fig. 1 with four sensor hoses each corresponding to its own chamber. We then introduced and tested continuously sliding and rotating control strategies to

<sup>1</sup> Embodied Dexterity Group, Dept. of Mechanical Engineering, University of California Berkeley, Berkeley, CA, USA. (email: jungpyo-lee@berkeley.edu; hstuart@berkeley.edu)

<sup>2</sup> The Dept. of Mechanical and Automation Engineering, T-Stone Robotics Institute, The Chinese University of Hong Kong, Hong Kong, China. (email: zhengsun@link.cuhk.edu.hk; zhipengdong@cuhk.edu.hk; feichen@cuhk.edu.hk)

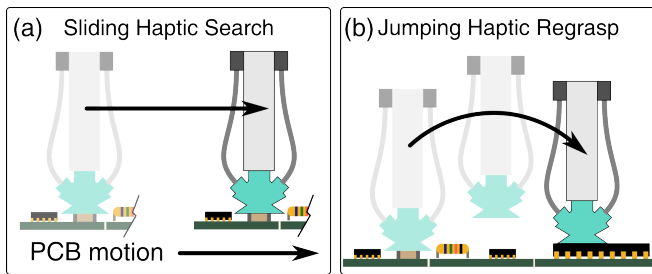


Fig. 2: (a) In sliding haptic search, the object can slide with the gripper, making the strategy ineffective at leading to a successful grasp. (b) We study the utility of jumping haptic regrasp to find a better grasp location without sliding continuously across the object’s surface.

haptically search for graspable object locations in [8]; we found that this strategy can improve grasping of adversarial objects by up to 2.52x during bin picking. However, the sliding haptic search method was shown to fail when the object moves along with the gripper, such that the relative position with the suction cup remains unchanged as depicted in Fig. 2(a). While we demonstrated continuous sliding haptic search with a PCB in this prior work, the PCB was rigidly fixed to the table to prevent it from moving with the cup. We now introduce and test the use of jumping haptic regrasp as a viable alternative for preventing sliding failure with loose PCB handling – this involves releasing and regrasping the object at a new location, as seen in Fig. 2(b). In the present work, we also update the implementation of the end-effector assembly for easier mechanical integration with existing robotic manipulation systems.

## B. Overview

Section II provides a description of the Smart Suction Cup with an updated end effector implementation. We also define the tested jumping haptic regrasp method that utilizes the pressure readings from each chamber to improve grasping on PCBs. In Section III, we categorize PCBs into two levels according to their recycling status and perform two discrete experimental pick-and-place tests with this system – one test is for PCB’s on a stationary table and the other is on a moving conveyor belt system and a realistic vision-based grasp planner. Section IV presents the results of these experiments; we find that the use of jumping regrasp increases the success rate in both pick-and-place applications, and that haptically-guided regrasp is useful especially in non-processed waste PCBs with the largest surface features. Discussed in Section V, transferring the haptic regrasp to real application encounters emerging issues that can be further improved in future work. We conclude that the jumping haptic method exhibits promising capabilities as corrective reflexes that complement traditional vision-based grasp planning approaches.

## II. JUMPING HAPTIC REGRASP IMPLEMENTATION

### A. End-Effector Hardware

In our prior work [7], [8], we provided comprehensive details regarding the fabrication, internal structure, and dimen-

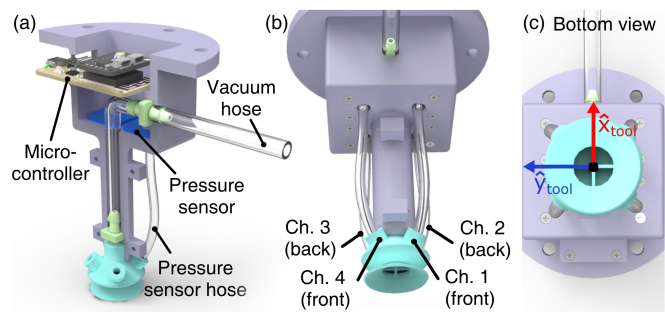


Fig. 3: CAD images for the suction cup system. (a) Sectional view of the system showing four pressure sensors and a microcontroller for data acquisition. Assembled system showing vacuum hose and pressure sensor hoses. (b) Configuration of four channels and the coordinate of tool frame. (c) Axes are aligning with the inner chamber’s walls, as illustrated in the bottom view.

sions of the suction cups. To briefly summarize, these suction cups are fabricated using a customized mold, resulting in a specialized design with an internal structure comprising four identical chambers for the purpose of airflow monitoring. The manufactured suction cup is integrated into the underside of a 3D-printed fixture, as shown in Fig. 3(a). In this paper, we have made slight updates to the end-effector for the Smart Suction Cup to simplify its integration onto various robot arms. These updates include a newly designed fixture, a new microcontroller, and a multiplexer for communication with sensors. All electronic components required for pressure measurements are newly enclosed within this fixture, including four pressure sensors (MPRLS, Adafruit) securely affixed to the internal space facing the bottom. These sensors are connected to the four chambers through polyurethane tubes. Also updated in the current design, the pressure sensors are linked to an I2C multiplex (PCA9546, Adafruit), which interfaces with the microcontroller (ESP32-S3 feather, Adafruit). The microcontroller is securely fastened to the fixture, and positioned on the opposite side of the main vacuum hose. The vacuum hose is attached to a barbed tube fitting positioned on the fixture’s side wall, with a hose extending through the fixture’s guide hole to the suction cup, completing the integrated system.

### B. Jumping Haptic Regrasping Algorithm

The aim of the haptic search controller is to adjust the end-effector pose of the robot arm until the suction cup becomes sealed against the surface. When this occurs, pressure sensors reach vacuum pressure levels, i.e. no flow conditions. We assume that the vacuum force is enough to lift any of the lightweight PCBs used in this study. During the haptic search, the robot conducts lateral pose adjustment to find a ‘good’ spot for grasping.<sup>1</sup> The direction for adjustment is calculated by the pressure difference between 4 channels, as seen in Fig. 3(b), at each grasping point. In order to calculate the pressure difference, we first define the vacuum pressure of each chamber as  $P_N = P_{atm} - P_{Ch.N}$  where

<sup>1</sup>While a smooth surface without via holes provides a suction seal, there are also good locations where chips or vias remain under the gripper.

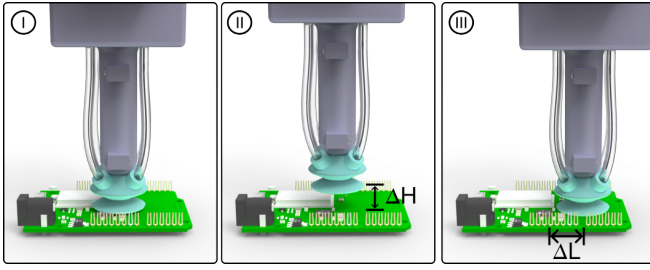


Fig. 4: Schematic CAD image of jumping haptic regrasp.

$N = [1, 2, 3, 4]$  is the chamber number,  $P_{atm}$  is atmospheric pressure, and  $P_{Ch.N}$  is the pressure reading from chamber  $N$ . A motion direction vector,  $v$ , is calculated as:

$$\vec{v} = ((P_1 + P_4) - (P_2 + P_3))\hat{x}_{tool} + ((P_3 + P_4) - (P_1 + P_2))\hat{y}_{tool} \quad (1)$$

to move towards the chambers with more vacuum pressure. We only consider the direction, not magnitude, of the pressure differences to move in the direction of the unit vector  $\hat{v} = \vec{v} / \|\vec{v}\|$ . We apply a threshold condition during the unit vector calculation, representing the noise floor of the pressure readings.<sup>2</sup> If the vacuum pressures from all chambers are below the threshold, the direction vector is set to  $\vec{v} = \vec{0}$ .

We employ a technique which we call ‘‘jumping haptic regrasp’’ (Fig. 4), during which the vacuum source is always ON. In this algorithm, the suction cup first approaches the object in an attempt to grip the PCB (I); it collects pressure information when in the target grasp position<sup>3</sup> to compute  $\hat{v}$ .<sup>4</sup> The robot arm then attempts to lift the PCB (II). Once the height of the gripper is lifted to  $\Delta H$  above the grasp position, the pressure is again measured to detect whether the grasp was successful or not.<sup>5</sup> If unsuccessful, then the cup moves to a new position above the PCB, with a lateral step size  $\Delta L$  (III), such that:

$$(x_{k+1}, y_{k+1}) = (x_k, y_k) + \Delta L \hat{v}(k) \quad k = 0, 1, 2, \dots \quad (2)$$

where  $\hat{v}(k)$  is the unit direction vector. For haptic search driven by the pressure readings of the Smart Suction Cup, we compute  $\hat{v}(k)$  using the measurements at  $(x_k, y_k)$  and Equation 1. As an alternative experimental control case, we also conduct a random jumping search in which the unit direction vector  $\hat{v}(k)$  in Equation 2 is chosen at random.

In the experiments conducted for this paper, we set  $\Delta H$  to 15 mm and  $\Delta L$  to 5 mm as selected through pilot testing.  $\Delta H$  is selected in order to avoid interference with protruding components on PCBs.  $\Delta L$  is selected in order to adjust the suction cup pose with the size of a single chamber. In order to find the initial grasp point  $(x_0, y_0)$ , we use a vision system

<sup>2</sup>The threshold is 10 Pa for the tabletop test, and 18 Pa for the conveyor belt system.

<sup>3</sup>The target grasp height is constant across all grasp attempts, a hardcoded value selected to make the cup lip flush with a flat PCB surface.

<sup>4</sup>The arm pauses for 50 ms to collect this data.

<sup>5</sup>Unsuccessful grasps are detected when the average of all chamber vacuum pressures is  $< 2000$  Pa. Likewise a successful grasp is when average pressure is  $> 2000$  Pa in the lifted pose.

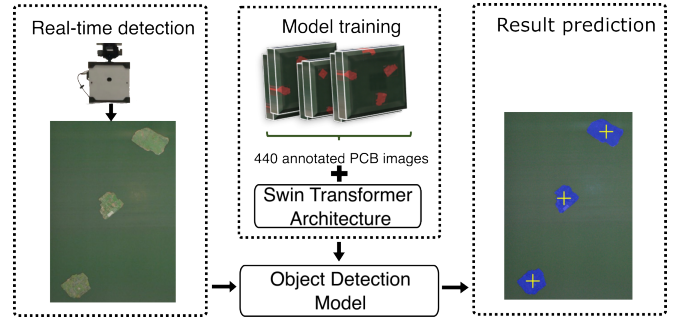


Fig. 5: PCB detection using mechanical learning: We used 440 fully annotated PCB images as the dataset to train the PCB object detection model. We use it to achieve the PCB real-time detection. The PCB’s location and its initial grasping point are predicted by the model.

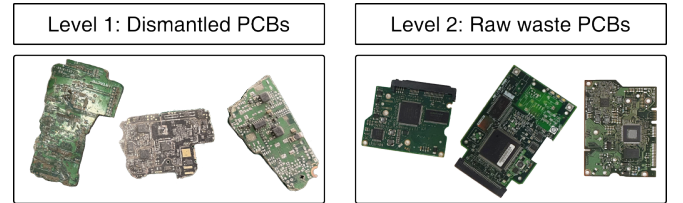


Fig. 6: PCB categories according to difficulty levels

where to segment PCBs from the image and calculate a center point.

### III. EXPERIMENTAL METHODS

#### A. Initial Grasp Position With Visual Segmentation

Data-driven vision approaches have been successfully applied to robot grasping planning [18]. The object recognition task involves object detection and semantic segmentation parts [19]. Beginning with the Swin Transformer architecture [20], transformer-based models have become the state-of-the-art object detection model. Hence, we utilize MMLab’s MMDetection toolbox [21] to help us train a Swin Transformer object detection model to localize and segment PCB objects for the subsequent grasping point estimation (Fig. 5). We use 440 fully annotated RGB images of PCBs as the dataset to train the model. This dataset is designed to recognize different types of PCBs and predict their segmentation area and accurate edge with minimal error [22]. To annotate PCBs, we first use the Segment Anything Model (SAM) [23] to segment a rough area and use coco-annotator [24] to refine and accurately annotate them. The initial grasping point is derived from the segmentation results. Upon obtaining the predicted semantic segmentation mask, we can acquire its contour line points set  $X$ , composed of  $n$  points, with the assistance of OpenCV library [25]. The empirical mean of the contour line points set  $X$  is selected as the initial grasping point  $(x_0, y_0)$ :

$$(x_0, y_0) = \frac{1}{n} \sum_{i=1}^n X. \quad (3)$$

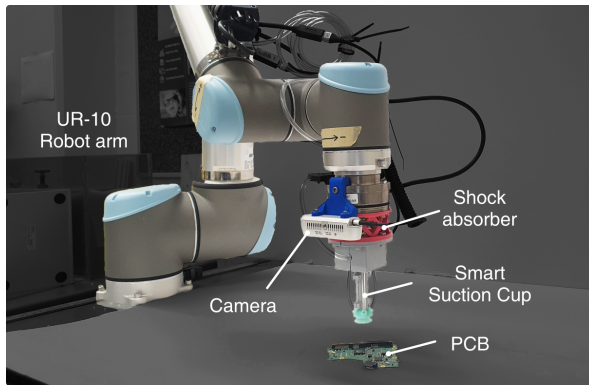


Fig. 7: Experimental setup for the pick and place test on the tabletop system.

### B. PCB Categories

To assess the effectiveness of our jumping haptic search method, we classify PCBs into two distinct difficulty levels based on their recycling status and surface complexity [1], [26], as illustrated in Fig. 6:

- 1) Level 1: Disassembled PCBs. These PCBs are processed using a mechanical dismantling machine, resulting in baseplate PCBs with little or no surface features. Baseplates may be warped by the dismantling process.
- 2) Level 2: Raw waste PCBs. These non-processed PCBs retain electronic components and are expected to pose a challenge for gripping using a suction cup.

Because Level 1 objects have been pre-processed, they have already been sorted out from other waste types at an earlier stage. However, we include both Levels in the current work because both may be present across varied applications, and Level 1 PCBs may still have surface features – vias, residual solder, warping, etc. – that hinder suction picking.

### C. Tabletop Evaluation for PCB Haptic Regrasping

We establish a tabletop task involving the picking-up of PCBs to assess the performance of our proposed jumping haptic regrasping, as depicted in Fig. 7. The tabletop experiments are conducted using a desktop computer running Ubuntu 20.04, equipped with a Ryzen 5700X CPU and NVIDIA RTX 3090 GPU. We employ Robot Operating System (ROS, Noetic) to gather pressure sensor data and command the UR-10 robot to reach target poses. An RGB-D camera (Intel RealSense D435) is mounted on the robot arm’s wrist, capturing photos at a resolution of 640x480 RGB, which are utilized for PCB segmentation. Additionally, we introduce a 3D-printed shock absorber made of TPU, strategically positioned between the robot arm and the suction cup system. This shock absorber serves to prevent the suction cup from exerting excessive force on electronic components as the height of surface mount components varies.

The robot system is programmed to employ either the haptic or random regrasping. Prior to commencing each grasping trial, the operator places a PCB on the tabletop with a random orientation. Subsequently, the robot attempts to grasp the PCB without researcher interference. First, the robot moves to an initial location to capture a photograph of the tabletop. After obtaining positional information from

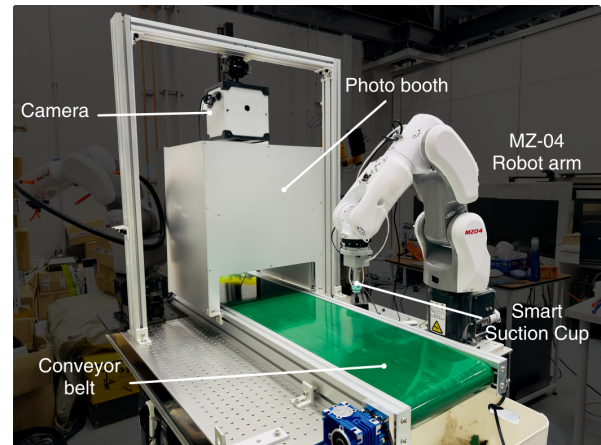


Fig. 8: Experimental setup for tests on a miniaturized conveyor belt system.

the visual segmentation, the robot approaches the target pose with a 15 mm height offset. It then starts the process of jumping regrasping, as described in Fig. 4. The robot continues to jump until either a successful grasp is achieved or the time limit of 10 seconds is reached. Following each trial, regardless of success or failure, the researcher removes the PCB and replaces it with a new PCB for the next trial.

### D. Demonstration on Conveyor Belt System

To emulate an industrial recycling setup, we test PCBs grasping on a miniaturized industrial conveyor belt system, as illustrated in Fig. 8. The conveyor belt, measuring 0.4 meters in width and 1.5 meters in length, is placed on a table and powered by a 220V DC motor (120RGU-CF, TAITUO Technology). We integrate a 6-axis robotic arm (MZ-04, Nachi Robotics) to perform pick-and-place. The input end of the conveyor belt features a vision system comprising a photo booth equipped with white lights and an RGB camera (MV-SUA501GC-T, MindVision).<sup>6</sup> The open-loop speed of the conveyor belt is set to 94 mm/s at all times, without pause. Thus, to monitor the speed and absolute movement distance of the conveyor belt, we employ an encoder (E6B2-CWZ6C 2000PR, OMRON). The smart suction cup is attached to the robotic wrist. We establish a workspace measuring 0.53 meters in length, considering the robot arm’s graspable area on the conveyor belt plane. Our computational setup consists of a desktop PC running Ubuntu 20.04, equipped with an NVIDIA 3060 graphics card, all managed by the Robot Operating System (ROS, Noetic) for model inference and robot control. Prior to conducting experiments, we perform calibration to determine the camera’s position and orientation relative to the end-effector, adjusted for the conveyor belt’s position using hand-eye calibration methods [27].

For each trial, the operator first places a PCB at the input of the conveyor belt with a random orientation. As the PCB traverses the belt and becomes visible to the camera, its segmentation mask and initial grasp point are predicted.<sup>7</sup>

<sup>6</sup>The camera captures images at a rate of 5 Hz.

<sup>7</sup>If a segmentation result indicates that the same PCB detected in the previous image is still present, the robot system disregards the result.

Once the initial grasping point is estimated, the robot moves to the starting line of the workspace with the predicted location, waiting for the PCB to pass directly beneath the suction cup. Subsequently, the robot commences jumping search on the PCB surface and continues until it successfully grips the PCB or reaches the end of the workspace on the conveyor belt. If the suction cup successfully grasps the PCB, the robot moves it to a designated location and released the PCB into a container.

Throughout the pick-and-place task, the robot continuously monitors the conveyor belt's speed and absolute location to ensure that the updated pose accurately reflects the relative location on the belt. The jumping search algorithm is modified from Equation 2 to include a compensation term representing the relative movement of the conveyor:

$$\Delta D = d_{k+1} - d_k \quad k = 0, 1, 2 \dots \quad (4)$$

$$(x_{k+1}, y_{k+1}) = (x_{k+1}, y_{k+1} + \Delta D) \quad (5)$$

where  $d_k$  represents the conveyor's absolute location when the robot is approaching the location  $(x_k, y_k)$ . During system setup, we aligned the direction of the conveyor with the robot's y-axis, such that we add the  $\Delta D$  on the  $y_{k+1}$  to ensure accurate pose updating.

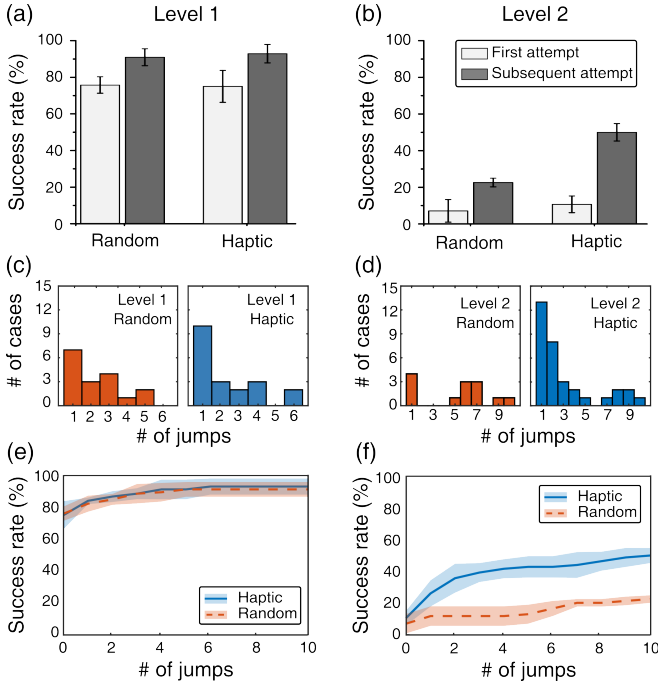


Fig. 9: The results of pick-and-release from the table top experiment. The success rates for random and haptic regrasping with (a) level 1 and (b) level 2 PCBs. Lighter gray bars are the success rate from an initial attempt and darker gray bars are the increased success rate with subsequent jumping regrasping. Histograms for the number of cases according to the number of jumps for each type with (c) level 1 and (d) level 2 PCBs. The success rate changes according to the number of jumps with (e) level 1 and (f) level 2 PCBs. Data are presented as the mean  $\pm$  s.d.

## IV. RESULTS

### A. Table-Top Pick and Release Test

The tabletop pick-and-release results are conducted for Level 1 PCBs (28 PCBs, 4 trials each) and Level 2 PCBs (21 PCBs, 4 trials each), presented in Fig. 9. For Level 1 PCBs, the random regrasping increases the success rate from  $75.9 \pm 4.5\%$  to  $91.1 \pm 4.6\%$  (Fig. 9a). The haptic regrasping exhibits a similar result with the success rate increasing from  $75.0 \pm 8.7\%$  to  $92.9 \pm 5.1\%$ . For the Level 2 PCBs (Fig. 9b), the initial attempts show lower success rates on the order of only 10%. While the random regrasping method only improved performance to  $22.6 \pm 2.4\%$ , the haptically-driven regrasping increases success to  $50.0 \pm 4.8\%$  representing a 370% performance increase.

Histograms depict the number of jumps required to achieve a successful grasp in each scenario (Fig. 9c, d). For Level 1 objects, the initial grasp is usually successful, and the grasp is likely to succeed with few additional grasps whether random or haptic control is used. However, in the case of Level 2 objects the chance of randomly finding a good grasp point is lower. Thus, only 4 cases are successfully gripped by random jumping within the first two regrasps. In contrast, haptic regrasping achieves 13 successes on the first regrasp and 8 cases on the second regrasp.

The overall trial success rate changes with respect to the number of jumps, depicted in Fig. 9e, f. For Level 1 PCBs, the success rate changes are nearly identical between random and haptic regrasping. However, as shown in Fig. 9f, haptic regrasping exhibits a logarithmic increase up to about 4 jumps, while random jumping shows a linear increase as the number of jumps increases. The effect of using haptically-driven direction estimation, as compared with random, appears most consequential for the first couple jumps.

### B. Demonstration on Conveyor Belt System

The results of the pick-and-place tests conducted on the conveyor belt system for Level 1 (52 PCBs, 4 trials each) PCBs and Level 2 PCBs (21 PCBs, 4 trials each) are presented in Fig. 10. For Level 1 PCBs (Fig. 10a), the random regrasping shows the success rate at the initial attempt is  $68.6 \pm 5.5\%$ , which increases to  $78.4 \pm 5.5\%$ . The haptic regrasping demonstrates a success rate increase from  $67.8 \pm 4.8\%$  to  $84.6 \pm 6.8\%$ . While the random regrasping shows a 14.4% performance increase, a 25.0% performance increase is achieved with the haptically-driven regrasping. For the Level 2 PCBs (Fig. 10b), the initial attempt presents a success rate of  $9.5 \pm 5.5\%$ , which increases to  $22.6 \pm 7.3\%$  with the random regrasping method. The haptically-driven regrasping increases the success rate from  $9.5 \pm 6.7\%$  to  $26.2 \pm 4.8\%$ . Performance increases by 134% and 176% for the random and haptic regrasping, respectively.

Histograms of successful grasping cases with respect to the number of jumps for each type are depicted in Fig. 10c, d. For the Level 1 PCBs, most successful grasps occur in the early stages of jumps in both cases, resulting in histograms that exhibit a plateauing trend. While, haptically-driven jumps show a higher number of successful cases, the

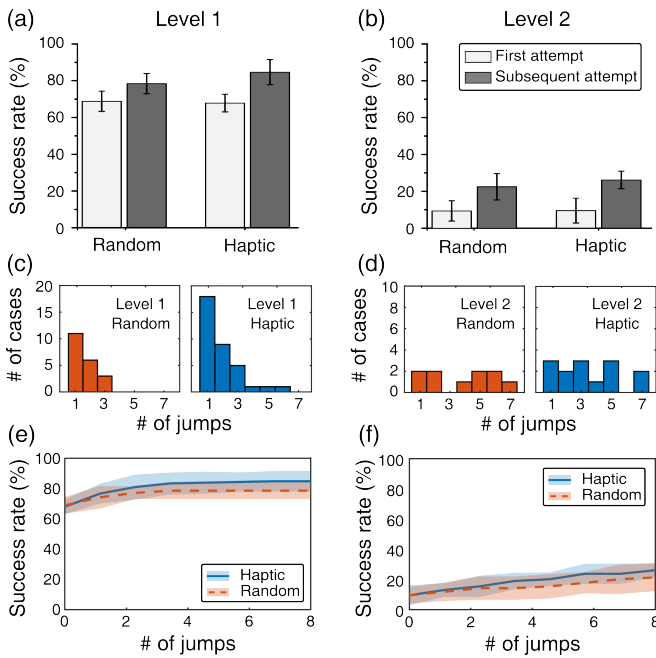


Fig. 10: The results of pick and place tasks on the conveyor belt system. The success rate for random and haptic regrasping for each type with (a) level 1 and (b) level 2 PCBs. Histograms for the number of cases according to the number of jumps for random and haptic regrasping for each type with (c) level 1 and (d) level 2 PCBs. The success rate changes according to the number of jumps for each type with (e) level 1 and (f) level 2 PCBs. Data are presented as the mean  $\pm$  s.d.

difference with random search is small. In the case of Level 2 objects, both the random and haptic search show evenly distributed chances of finding a good grasp point. These trends are also shown in success rate changes (Fig. 10c, d); the success rate increases slightly faster in haptic regrasping, and keeps increasing slowly after the first three jumps for the Level 1 PCBs, while the success rate gradually increase in the case of Level 2 PCBs.

## V. DISCUSSION

We evaluated the performance of the proposed jumping haptic regrasping on the tabletop experimental setup. For table-top tests, we observed that the difficulty of the object to be gripped correlated with a more substantial performance improvement achieved through haptic regrasping, as compared with random search. In other words, haptic information is beneficial for the suction cup to regrasp more complex objects, like Level 2 PCBs. Interestingly, obstacles that prevent the suction cup from engaging with surfaces can help the system discern pressure differences between chambers, enabling the suction cup to know where to go for a better grasp. For instance, some PCBs have flat components such as microprocessors, which represent an ideal point for the suction cup to grip. If the suction cup touches the edge of the microprocessor, it tends to move in the direction of the microprocessor, even though this obstacle prevents it from grasping initially. In comparison, random jumps do not guarantee finding this prospective grasp point.

Although our regrasping algorithm enhances the probability of successful grasp on PCBs, the success rate doesn't

reach 100% even for level 1 PCBs. This can be explained by failure cases discussed in the prior work [8]. One common failure mode is that an initial grasp point can be located in an area where there are a lot of electronic components, thereby it is impossible to be gripped in that region by the suction cup. The other common failure case is haptic oscillation, where the suction keeps moving back and forth without a successful grasp. One possible solution for this haptic oscillation is to use various step sizes ( $\Delta L$ ) from the pressure readings. Future work will include an adaptive choice of this parameter, which could be informed by further understanding of air flows on complex PCB surfaces.

Conducting robotic demonstrations in an industrial setup is crucial to translate manipulation methods initially developed in a laboratory environment. Thus, we evaluated our system using a scaled-down industrial conveyor belt setup. In these trials we find the null result: inconsequential differences between random and haptic regrasping methods on both Level 1 and 2 PCBs. The positive results from Level 2 table-top tests do not translate to the conveyor application in the current implementation. As of now, jumping haptic regrasp is only helpful when the object remains stationary.

Transitioning robotics technology from research labs to industrial settings faces challenges due to the lab-to-industry gap [28]. This transition often involves adapting experimental setups with strictly controlled conditions to real-world industrial environments, which can introduce new complexities and uncertainties. We suspect the null outcome is in part due to relative motion between the cup and conveyor that unintentionally displaces the object, negating haptic information. In the tabletop experiment, the suction cup only moves vertically relative to the PCB during grasping. However, a short pause of the suction cup at the target grasp position to collect pressure data was observed to result in unwanted pose changes of PCBs due to the conveyor belt's motion. These disturbances likely decrease haptic regrasp direction estimate effectiveness. This essentially led to a haptic regrasp attempt resembling a random jump. To address these challenges, future work will incorporate real-time tracking of PCB orientations with a wrist-mounted camera to enable haptic regrasping between jumps that compensate for PCB motions.

## VI. CONCLUSION

In this study, we presented a jumping haptic regrasping for determining a searching direction with the Smart Suction Cup. This approach enables the suction cup to adjust its pose for more successful suction grasping of stationary Level 2 PCBs, with surface features difficult to capture by a vision-based planner. With ongoing development, the Smart Suction Cup is a promising tool for recycling sorting applications involving objects with intricate surface features, like PCBs.

## ACKNOWLEDGEMENT

This work is supported by InnoHK of the Government of the Hong Kong Special Administrative Region via the Hong Kong Centre for Logistics Robotics.

## REFERENCES

- [1] X. Zeng, L. Zheng, H. Xie, B. Lu, K. Xia, K. Chao, W. Li, J. Yang, S. Lin, and J. Li, "Current status and future perspective of waste printed circuit boards recycling," *Procedia Environmental Sciences*, vol. 16, pp. 590–597, 2012.
- [2] J. Li, P. Shrivastava, Z. Gao, and H.-C. Zhang, "Printed circuit board recycling: a state-of-the-art survey," *IEEE transactions on electronics packaging manufacturing*, vol. 27, no. 1, pp. 33–42, 2004.
- [3] S. B. Wath, A. N. Vaidya, P. Dutt, and T. Chakrabarti, "A roadmap for development of sustainable e-waste management system in india," *Science of the Total Environment*, vol. 409, no. 1, pp. 19–32, 2010.
- [4] J. Li, B. Tian, T. Liu, H. Liu, X. Wen, and S. Honda, "Status quo of e-waste management in mainland china," *Journal of Material Cycles and Waste Management*, vol. 8, pp. 13–20, 2006.
- [5] R. Khanna, R. Cayumil, P. Mukherjee, and V. Sahajwalla, "A novel recycling approach for transforming waste printed circuit boards into a material resource," *Procedia environmental sciences*, vol. 21, pp. 42–54, 2014.
- [6] Y. Lu, B. Yang, Y. Gao, and Z. Xu, "An automatic sorting system for electronic components detached from waste printed circuit boards," *Waste Management*, vol. 137, pp. 1–8, 2022.
- [7] T. M. Huh, K. Sanders, M. Danielczuk, M. Li, Y. Chen, K. Goldberg, and H. S. Stuart, "A multi-chamber smart suction cup for adaptive gripping and haptic exploration," in *2021 IEEE/RSJ International Conference on Intelligent Robots and Systems (IROS)*. IEEE, 2021, pp. 1786–1793.
- [8] J. Lee, S. D. Lee, T. M. Huh, and H. S. Stuart, "Haptic search with the smart suction cup on adversarial objects," *IEEE Transactions on Robotics*, vol. 40, pp. 226–239, 2024.
- [9] A. Jaiswal and B. Kumar, "Vacuum gripper-an important material handling tool," *Int J Sci Technol*, vol. 7, pp. 1–8, 2017.
- [10] Y. Yoo, J. Eom, M. Park, and K.-J. Cho, "Compliant suction gripper with seamless deployment and retraction for robust picking against depth and tilt errors," *IEEE Robotics and Automation Letters*, vol. 8, no. 3, pp. 1311–1318, 2023.
- [11] E. Papadakis, F. Raptopoulos, M. Koskinopoulou, and M. Maniadakis, "On the use of vacuum technology for applied robotic systems," in *2020 6th International Conference on Mechatronics and Robotics Engineering (ICMRE)*. IEEE, 2020, pp. 73–77.
- [12] D. Pham and S. Ye, "Strategies for gripper design and selection in robotic assembly," *The International Journal of Production Research*, vol. 29, no. 2, pp. 303–316, 1991.
- [13] F. Raptopoulos, M. Koskinopoulou, and M. Maniadakis, "Robotic pick-and-toss facilitates urban waste sorting," in *2020 IEEE 16th International Conference on Automation Science and Engineering (CASE)*. IEEE, 2020, pp. 1149–1154.
- [14] J. Mahler, M. Matl, V. Satish, M. Danielczuk, B. DeRose, S. McKinley, and K. Goldberg, "Learning ambidextrous robot grasping policies," *Science Robotics*, vol. 4, no. 26, p. eaau4984, 2019.
- [15] B. Sauvet, F. Lévesque, S. Park, P. Cardou, and C. Gosselin, "Model-based grasping of unknown objects from a random pile," *Robotics*, vol. 8, no. 3, p. 79, 2019.
- [16] S. P. Gundupalli, S. Hait, and A. Thakur, "A review on automated sorting of source-separated municipal solid waste for recycling," *Waste management*, vol. 60, pp. 56–74, 2017.
- [17] J. Mahler, M. Matl, X. Liu, A. Li, D. Gealy, and K. Goldberg, "Dexnet 3.0: Computing robust vacuum suction grasp targets in point clouds using a new analytic model and deep learning," in *2018 IEEE International Conference on robotics and automation (ICRA)*. IEEE, 2018, pp. 5620–5627.
- [18] R. Newbury, M. Gu, L. Chumbley, A. Mousavian, C. Eppner, J. Leitner, J. Bohg, A. Morales, T. Asfour, D. Kragic, *et al.*, "Deep learning approaches to grasp synthesis: A review," *IEEE Transactions on Robotics*, 2023.
- [19] L. Yu and M. T. Orchard, "Accurate edge location identification based on location-directed image modeling," in *2019 IEEE International Conference on Image Processing (ICIP)*. IEEE, 2019, pp. 2971–2975.
- [20] Z. Liu, Y. Lin, Y. Cao, H. Hu, Y. Wei, Z. Zhang, S. Lin, and B. Guo, "Swin transformer: Hierarchical vision transformer using shifted windows," in *Proceedings of the IEEE/CVF international conference on computer vision*, 2021, pp. 10 012–10 022.
- [21] K. Chen, J. Wang, J. Pang, Y. Cao, Y. Xiong, X. Li, S. Sun, W. Feng, Z. Liu, J. Xu, Z. Zhang, D. Cheng, C. Zhu, T. Cheng, Q. Zhao, B. Li, X. Lu, R. Zhu, Y. Wu, J. Dai, J. Wang, J. Shi, W. Ouyang, C. C. Loy, and D. Lin, "MMDetection: Open mmlab detection toolbox and benchmark," *arXiv preprint arXiv:1906.07155*, 2019.
- [22] L. Yu and M. T. Orchard, "Location-directed image modeling and its application to image interpolation," in *2018 25th IEEE International Conference on Image Processing (ICIP)*. IEEE, 2018, pp. 2192–2196.
- [23] A. Kirillov, E. Mintun, N. Ravi, H. Mao, C. Rolland, L. Gustafson, T. Xiao, S. Whitehead, A. C. Berg, W.-Y. Lo, *et al.*, "Segment anything," *arXiv preprint arXiv:2304.02643*, 2023.
- [24] J. Brooks, "COCO Annotator," <https://github.com/jsbrooks/coco-annotator/>, 2019.
- [25] G. Bradski, "The OpenCV Library," *Dr. Dobb's Journal of Software Tools*, 2000.
- [26] J. Cui and E. Forsberg, "Mechanical recycling of waste electric and electronic equipment: a review," *Journal of hazardous materials*, vol. 99, no. 3, pp. 243–263, 2003.
- [27] A. Tabb and K. M. Ahmad Yousef, "Solving the robot-world hand-eye (s) calibration problem with iterative methods," *Machine Vision and Applications*, vol. 28, no. 5-6, pp. 569–590, 2017.
- [28] G. Vekinis, "Out into the real world: Scaling up," in *Mastering Technology Transfer: From Invention to Innovation: A Step-by-Step Guide for Researchers and Inventors*. Springer, 2023, pp. 141–161.